Stratovolcano growth by co-eruptive intrusion: The 2008 eruption of Tungurahua Ecuador

J. Biggs,[1,2,3] P. Mothes,[4] M. Ruiz,[4] F. Amelung,[2] T. H. Dixon,[2] S. Baker,[2] and S-H. Hong[2]

Received 30 July 2010; revised 6 September 2010; accepted 13 September 2010; published 3 November 2010.

[1] Volcanic edifices are constructed by a combination of erupted material and internal growth. We use the L-band satellite ALOS to produce InSAR measurements at Tungurahua Volcano, Ecuador. We find a maximum of 17.5 cm of uplift on the upper western flank between December 2007 and March 2008, coincident with an eruption in February 2008. The deformation can be modeled using an ellipsoidal or sill-like source within the edifice. The models require an elongated aspect ratio with a length of 4–6 km. The intruded volume of 1.2×10^6 m^3 is roughly equivalent to the bulk erupted volume of 1.5×10^6 m^3 and together the values are roughly equal to the long-term magma flux. The question remains whether this uplift is permanent, thus contributing to the internal growth of the edifice, or temporary, in which case the magma will be released in a future eruption. **Citation:** Biggs, J., P. Mothes, M. Ruiz, F. Amelung, T. H. Dixon, S. Baker, and S.-H. Hong (2010), Stratovolcano growth by co-eruptive intrusion: The 2008 eruption of Tungurahua Ecuador, *Geophys. Res. Lett.*, *37*, L21302, doi:10.1029/2010GL044942.

1. Introduction

[2] Tungurahua is a steep-sided andesitic stratovolcano located in the Eastern Cordillera of the Ecuadorian Andes (Figure 1). We use Interferometric Synthetic Aperture Radar (InSAR) to study deformation patterns from 2006–2009, including the February 2008 eruptive period. We then propose a source model and compare the observations with seismicity and gas measurements in order to understand the physical development of the volcanic system during this period.

1.1. Mechanisms of Edifice Growth

[3] Both extrusive and internal growth contributes to the height and volume of volcanic edifices. Internal (endogenous) growth can take the form of dike or sill intrusions or cumulate formation. Internal growth has been directly observed during andestic and dacitic dome formation [e.g., *Kaneko*, 2002] and dike intrusions into basaltic shields [*Annen*, 2001] and in close association with explosive activity [*Newhall and Melson*, 1983]. Field observations of eroded volcanic edifices show that small-scale intrusions are found in zones of weakness such as sedimentary strata, the interfaces between lava flows as well as faults and fractures [*Mathieu and Van Wyk de Vries*, 2009].

[4] Stratovolcano edifices, including that of Tungurahua, Ecuador, are predominantly composed of erupted products: inter-bedded layers of lava, tephra and volcanic ash. Nonetheless, some gravity surveys reveal dense material suggesting the solidification of magma within the shallow plumbing system [*Locke*, 1997]. Episodes of uplift during periods of apparent quiescence may be common [e.g., *Lu et al.*, 2002; *Wicks et al.*, 2002] but given the quoted source depths of 6–7 km the preferred explanation is of temporary magma storage rather than growth of the edifice.

1.2. Tungurahua Volcano

[5] The western flank of Tungurahua is composed of unconsolidated avalanche debris, subsequent pyroclastic flows, tephra deposits and lavas to a depth of ~2 km [*Molina et al.*, 2004] following a collapse of the previous edifice 3000 years ago [*Hall et al.*, 1999]. Since colonial times, Tungurahua has experienced five eruptive periods: 1640–1641, 1773–1777, 1886–1888, 1916–1918 and 1999-present with compositions ranging from basaltic andesites to dacites [*Hall et al.*, 1999; *Le Pennec et al.*, 2008]. Recent growth in population, infrastructure and economic activity around Tungurahua Volcano raises concerns about hazards posed by future eruptions.

[6] The current period of unrest began in Oct-Dec 1999 and consisted of intermittent mild strombolian eruptions [*Ruiz et al.*, 2006]. Three eruptions on 14th July 2006, 16–17th August 2006 and 6–7th February 2008 produced widespread pyroclastic flows and ash falls, resulting in the loss of lives, repeated evacuation and damage to infrastructure [*Global Volcanism Program*, 2006]. Peaks in seismic and gas parameters preceded both 2006 eruptions and tiltmeter measurements have been interpreted as due to the formation of a bulge on the northern flank between 11–16th August [*Arellano et al.*, 2008; *Global Volcanism Program*, 2006; *Carn et al.*, 2008].

2. The 2008 Eruption

[7] Ground-based monitoring provides a detailed record of volcanological and geophysical observations leading up to the February 2008 eruption. A network of broad-band seismic and infrasound stations recorded heightened seismic activity beginning in August 2007. Events are classified according to *Ruiz et al.* [2006]: explosion events have short-duration pressure transients with an impulsive onset, while jetting tremors have emergent onsets with long-duration

[1]COMET, Department of Earth Sciences, University of Oxford, Oxford, UK.
[2]RSMAS, University of Miami, Coral Gables, Florida, USA.
[3]Now at Department of Earth Sciences, University of Bristol, Bristol, UK.
[4]Instituto Geofisico, Escuela Politenica Nacional, Quito, Ecuador.

0094-8276/10/2010GL044942

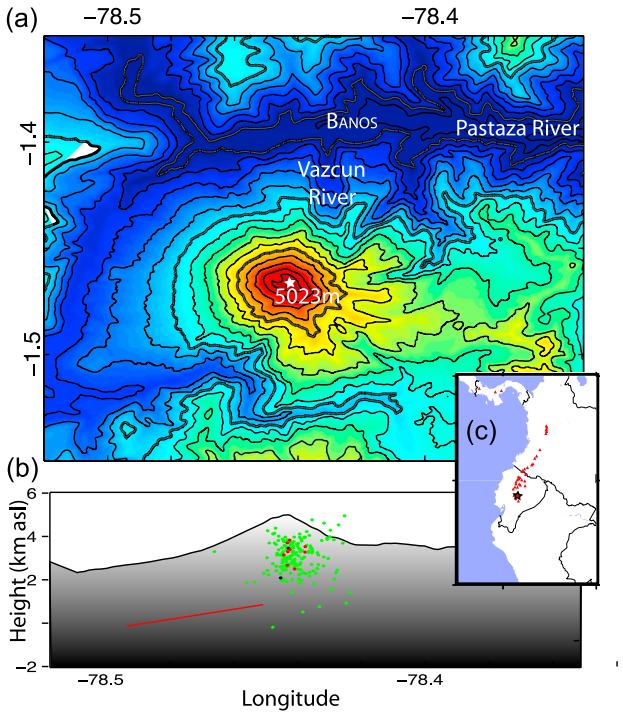

Figure 1. (a) Topography of Tungurahua Volcano Edifice. In historical eruptions, the deeply incised Vazcun valley has conducted lahars and pyroclastic flows directly towards the town of Banos (pop. 15,000) and the Agoyan hydroelectric dam on the Pastaza river. Contours every 200 m; thick contours every 1000 m. (b) East–West cross section. The best-fitting, topographically-corrected source (red line) is located within the volcanic edifice. Seismicity from July 2007 to January 2008, showing explosions (green), volcano-tectonic events (black) and long-period (red). (c) Location map: North Andean Volcanic Chain (triangles) and Tungurahua (star).

pressure codas. Of the 12,000 events of volcanic origin, most (59%) were identified as explosive due to the presence of infrasonic pulses arriving at the station a few seconds after the seismic signal. A large number of explosions (more than 100 per day) were recorded from 29 December up to the eruption onset with peaks that reached more than 300 explosions on 3 and 4 January, and 2 and 5 February. Very large vulcanian explosions (>500 Pa at 6 km distance) were recorded on 11,13 and 23 December, 2007. Few long-period seismic events were recorded, especially during the day preceding the eruption. Following the February 2008 eruption, the volcano entered a period of relative quiescence with only a few small explosions and jetting tremors recorded. Gas emissions increased from an average of 954 tons per day of SO_2 for the 60-day period before 5th February to an average of 1627 tons per day of SO_2 for the 60 days following the eruption (S. Hidalgo, personal communication, 2009).

[8] The total volume erupted during the 2007–2008 eruption was 1.7×10^6 m^3 (J. Bustillos, personal communication, 2009), composed of ash and pyroclastic flows. Isopachmaps developed from systematic ash sampling determined a maximum thickness of 3 mm extending out 13 km West of the crater from 30 January to 9 February with a volume of 8×10^5 m^3; continuing ash falls on 10–11 February produced a similar volume of 8×10^5 m^3. A small pyroclastic flow deposit from 6 February was found in one narrow ravine on the western flank and its volume is estimated at ~2×10^5 m^3.

3. InSAR Observations

[9] Interferometric Synthetic Aperture Radar (InSAR) uses repeat satellite images to produce a dense spatial map of ground deformation. InSAR has been extremely effective at imaging ground deformation at many shield volcanoes and calderas and is particularly useful at volcanoes in which ground-based observations are limited. However, InSAR observations at stratovolcanoes in the tropics are limited by: 1) dense vegetation cover causing decorrelation, 2) steep topography causing baseline-dependent geometric decorrelation and 3) seasonal variations in water vapour causing topographically-correlated phase shifts which are difficult to separate from ground deformation. These limitations have restricted the use of InSAR for measuring co-eruptive deformation during a number of significant eruptions [*Zebker et al.*, 2000]. Even when measurements are possible, stratovolcanoes frequently show no deformation even during periods of activity, a result which can be explained by an open system behavior at low flux rates [*Williams-Jones*, 2003]; a precise balance between pre- and post-eruptive displacements [*Moran et al.*, 2006] or a deep magma reservoir [*Pritchard and Simons*, 2004].

[10] The Japanese satellite ALOS was launched in January 2006 and operates an L-band SAR; longer-wavelength radar is less susceptible to vegetation and provides the first opportunity to make InSAR measurements at many volcanoes in the tropics. Between December 2006 and December 2009, ALOS acquired 13 radar images covering Tungurahau volcano providing 3 years of continuous observations. Due to steep slopes, snow cover and some large interferometric baselines, the top of the volcano is decorrelated in the many interferograms, but coherenceon the flanks is good.

[11] Deformation is visible in interferograms that span the period 26 December 2007 to 27 March 2008 (Figure 2) but no similar signature was observed prior to December 2007 or following March 2008 (Figure 3). The signal appears on the upper western flank and consists of a single lobe elongated east–west. Inspection of the interferograms in radar geometry show that the offset from the peak is not an artefact of the filtering or geocoding algorithms acting on

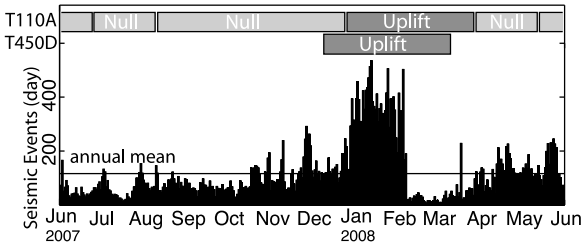

Figure 2. Ground based observations for the period June 2007–June 2008 showing a sustained period of seismicity related to vigorous explosive activity between 20th October 2007 and 5th February 2008. Ash falls began in late January, followed by pyroclastic flows.

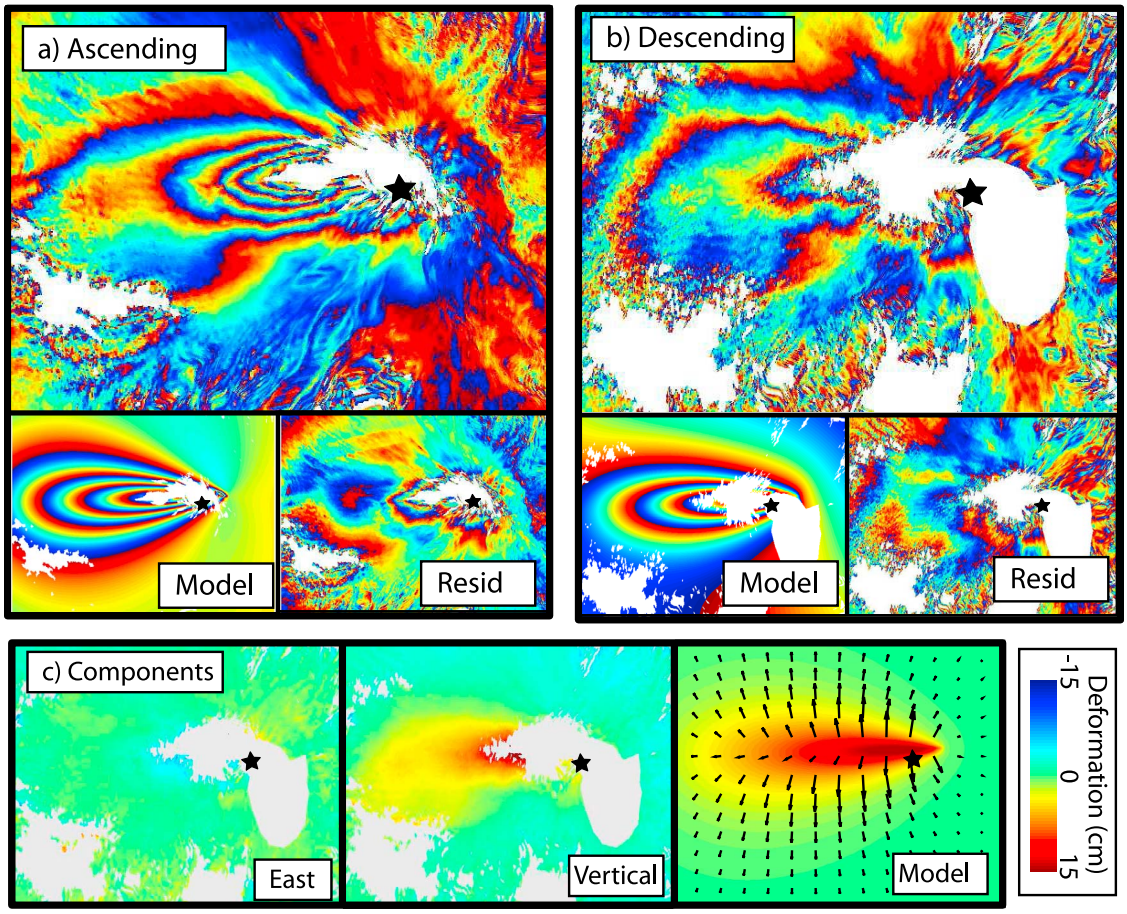

Figure 3. ALOS Interferograms spanning December 2007–March 2008. (a) Stack of two independent interferograms from an ascending line of sight. (b) Single interferogram from a descending line of sight. Both interferograms are re-wrapped to 2.8 cm fringes. (c) Deformation decomposed into east and vertical components respectively. The peak is 17.5 cm of uplift with little horizontal motion. Model displacement, from the elastic half-space model-colours represent vertical motion and arrows represent horizontal motion.

layover regions caused by the steep topography. Furthermore, the signal is offset to the west of the peak in both ascending and descending images, despite the opposing look directions.

[12] Combining observations from different look directions for the three-month period between December 2007 and March 2008, and making the assumption that the north–south component of motion has a negligible contribution to the interferogram shows that the motion is dominantly vertical with a maximum uplift of 17.5 cm (Figure 3).

[13] Gas emissions from Tungurahua merge to form a continuous tropospheric gas plume, which is most commonly directed westwards [*Carn et al.*, 2008]. Water vapour affects the radar path length and is likely to be a large proportion of the plume. Assuming that H_2O and SO_2 in the plume are correlated, we evaluated daily Ozone Mapping Instrument (OMI) measurements of SO_2 to assess the path delay for each radar acquisition. Despite variable levels of SO_2 there is no apparent correlation with the observed deformation. Likewise, ash and ballistic fallout occurs mainly on the volcano's upper western flank but based on the width of the inflationary lobe observed in the interferogram and the absence of notable deformation on the NW flank, where ballistics also fell, it is unlikely that accumulation of eruptive fallout during early 2008 has any bearing on the observed deformation pattern.

[14] The small diameter of the signal (<4 km) compared to the edifice diameter (~10–15 km) and absence of a phase change in other interferograms using these images, demonstrates that the signal is geodetic rather than the result of contamination by vertically stratified water vapour in the troposphere.

4. Deformation Source

[15] In order to model the observations, we explore a range of simple analytic models for deformation within an elastic half space. Point source or penny-shaped cracks [*Mogi*, 1958; *Fialko et al.*, 2001] produce circular deformation patterns which are inconsistent withthe elongated fringe pattern observed. Models of dike intrusion, including that proposed by *Fournier et al.* [2010], are dominated by horizontal motion and typically have two lobes [*Okada*, 1985], providing a poor fit.

[16] We find two model geometries which are capable of explaining the observations. The first is a prolate spheroid [*Davis and Dieterich*, 1988] with an extremely eccentric aspect ratio of 100:1. The long axis, oriented east–west, is

3.4 km long and plunges at 13° to the horizontal. The two shorter axes are ~ 40 m. The second is an elongated sill which is 4.8 km long dipping at 23°. The volume of intrusion is well-constrained (1.1×10^6 m^3) but the width and length trade off with little effect on the overall misfit - we chose a width of 200m and opening of 1.1 m. The misfits are 10.1 and 10.2 mm respectively. In both cases, the source depth is less than 1 km, located within the 3 km-high volcanic edifice and the geometry approximates a long tube or line source (Figure 1). Parameters, errors and trade-offs are given in Figures S1 and S2 of the auxiliary material.[1]

[17] Simple geometric corrections to account for topography [*Williams and Wadge*, 1998] provide useful approximations for moderate relief [*Cayol and Cornet*, 1998] but are not applicable in this extreme case. Instead, we use the method of *Williams and Wadge* [2000] which uses a series expansion of the elastic half-space solution with a small slope approximation, yielding a set of higher-order corrections. Using a grid search of the parameter space for a shallowly-dipping, elongated sill, we find extensive trade-offs (see Figure S3 of the auxiliary material) but the best-fitting sills are consistently at heights of 2900 m above sea level, still >2 km below the summit, and are at least 5.6 km in length (Figure 1).

5. Discussion and Conclusions

[18] The interferograms show that 17.5 cm of uplift occurred between 26 December 2007 and 27 March 2008, but it is not possible to determine whether this occurred steadily (weeks to months) or rapidly (hours to days). The interferograms cover the complete eruption cycle from pre-eruptive pressurization to post-eruptive relaxation (Figure 2). Thus we assume any deformation associated with transient changes in the magmatic plumbing system will have canceled out and the observed deformation must be permanent over a single eruption cycle. Further observations are required to determine if the magma storage is temporary or permanent in the longer term.

[19] The earthquake locations corresponding to the time period of the interferogram (dominantly explosions) do not correspond to the source model, indicating that the intrusion took place aseismically (Figure 1b). A larger sample of relocated volcano-tectonic events from 1999–2003, appear to show a sub-vertical structure within the edifice leaning to the west and a low-velocity zone under the western flank, the base of which corresponds roughly to our source model [*Molina et al.*, 2004].

[20] The volume of the volcanic edifice has grown internally by 1.2×10^6 m^3 during the eruption. The intruded volume (1.2×10^6 m^3) is similar to the erupted volume (1.5×10^6 m^3) indicating the cone grew in equal parts by intrusion and extrusion during this cycle. The total volume growth (the sum of the erupted and intruded volumes) is 2.7×10^6 m^3 – less than 1% of the volume required (3.1 km^3) to rebuild the previous cone of Tungurahua [*Hall et al.*, 1999]. Assuming this represents the magma supplied between the previous event (August 2006) and this eruption (February 2009) this gives a magma flux of 1.8×10^6 m^3/yr, which is surprisingly consistent with the long-term rate of 1.5×10^6 m^3/yr estimated from cone growth during the last 2300 years [*Hall et al.*, 1999].

[21] In the future, observations from InSAR and newly-installed GPS sites will test whether these observations are peculiar to this eruptive cycle or characteristic of the general behaviour. With a higher temporal sampling it may be possible to determine at which point during the eruptive cycle the intrusion occurs.

[22] **Acknowledgments.** We thank Tom Fournier and one anonymous reviewer. J.B. was supported by a Rosenstiel Fellowship at the University of Miami and a Changing Earth Science fellowship from ESA while at Oxford and Bristol. All ALOS data were acquired through WInSAR while at the University of Miami. Many thanks to Geoff Wadge and Susanna Ebmeier for their help with Topodef written by Charles Williams.

References

Annen, C. (2001), The long-term growth of volcanic edifices: Numerical modelling of the role of dike intrusion and lava-flow emplacement, *J. Volcanol. Geotherm. Res.*, *105*, 263–289, doi:10.1016/S0377-0273(00)00257-2.

Arellano, S. R., M. Hall, P. Samaniego, J. Le Pennec, A. Ruiz, I. Molina, and H. Yepes (2008), Degassing patterns of Tungurahua volcano (Ecuador) during the 1999–2006 eruptive period, inferred from remote spectroscopic measurements of SO_2 emissions, *J. Volcanol. Geotherm. Res.*, *176*, 151–162, doi:10.1016/j.jvolgeores.2008.07.007.

Carn, S. A., A. J. Krueger, S. Arellano, N. A. Krotkov, and K. Yang (2008), Daily monitoring of Ecuadorian volcanic degassing from space, *J. Volcanol. Geotherm. Res.*, *176*, 141–150, doi:10.1016/j.jvolgeores.2008.01.029.

Cayol, V., and F. H. Cornet (1998), Effects of topography on the interpretation of the deformation field of prominent volcanoes—Application to Etna, *Geophys. Res. Lett.*, *25*, 1979–1982, doi:10.1029/98GL51512.

Davis, P. M., and J. H. Dieterich (1988), Deformation from inflation of a dipping finite prolate spheroid in an elastic half-space as a model for volcanic stressing, *J. Geophys. Res.*, *93*, 4249–4257.

Fialko, Y., Y. Khazan, and M. Simons (2001), Deformation due to a pressurized horizontal circular crack in an elastic half-space, with applications to volcano geodesy, *Geophys. J. Int.*, *146*, 181–190, doi:10.1046/j.1365-246X.2001.00452.x.

Fournier, T. J., M. Pritchard, and S. Riddick (2010), Duration, magnitude, and frequency of subaerial volcano deformation events: New results from Latin America using InSAR and a global synthesis, *Geochem. Geophys. Geosyst.*, *11*, Q01003, doi:10.1029/2009GC002558.

Global Volcanism Program (2006), Tungurahua (Ecuador) intense ongoing activity in 2006: New bulge on the N flank, *GVN Bull.*, *31*, 2–4.

Hall, M., C. Robin, B. Beate, P. Mothes, and M. Monzier (1999), Tungurahua Volcano, Ecuador: Structure, eruptive history and hazards, *J. Volcanol. Geotherm. Res.*, *91*, 1–21, doi:10.1016/S0377-0273(99)00047-5.

Kaneko, T. (2002), Exogenous and endogenous growth of the Unzen lava dome examined by satellite infrared image analysis, *J. Volcanol. Geotherm. Res.*, *116*, 151–160, doi:10.1016/S0377-0273(02)00216-0.

Le Pennec, J., D. Jaya, P. Samaniego, P. Ramón, S. Moreno Yánez, J. Egred, and J. van der Plicht (2008), The AD 1300 1700 eruptive periods at Tungurahua volcano, Ecuador, revealed by historical narratives, stratigraphy and radiocarbon dating, *J. Volcanol. Geotherm. Res.*, *176*, 70–81, doi:10.1016/j.jvolgeores.2008.05.019.

Locke, C. (1997), Egmont Volcano, New Zealand: Three-dimensional structure and its implications for evolution, *J. Volcanol. Geotherm. Res.*, *76*, 149–161, doi:10.1016/S0377-0273(96)00074-1.

Lu, Z., C. Wicks, D. Dzurisin, J. A. Power, S. C. Moran, and W. Thatcher (2002), Magmatic inflation at a dormant stratovolcano: 1996–1998 activity at Mount Peulik volcano, Alaska, revealed by satellite radar interferometry, *J. Geophys. Res.*, *107*(B7), 2134, doi:10.1029/2001JB000471.

Mathieu, L., and B. Van Wyk de Vries (2009), Edifice and substrate deformation induced by intrusive complexes and gravitational loading in the Mull volcano (Scotland), *Bull. Volcanol.*, *71*, 1133–1148, doi:10.1007/s00445-009-0295-5.

Mogi, K. (1958), Relations between eruptions of various volcanoes and the deformations of the ground surfaces around them, *Bull. Earthquake Res. Inst.*, *36*, 99–134.

Molina, I., H. Kumagai, J. Le Pennec, and M. Hall (2004), Three-dimensional P-wave velocity structure of Tungurahua Volcano, Ecuador, *Eos Trans. AGU*, *85*(47), Fall Meet. Suppl., Abstract V11B-1427.

Moran, S. C., O. Kwoun, T. Masterlark, and Z. Lu (2006), On the absence of InSAR-detected volcano deformation spanning the 1995 1996 and

[1] Auxiliary materials are available in the HTML. doi:10.1029/2010GL044942.

1999 eruptions of Shishaldin Volcano, Alaska, *J. Volcanol. Geotherm. Res.*, *150*, 119–131, doi:10.1016/j.jvolgeores.2005.07.013.

Newhall, C., and W. Melson (1983), Explosive activity associated with the growth of volcanic domes, *J. Geophys. Res.*, *17*, 111–131, doi:10.1016/0377-0273(83)90064-1.

Okada, Y. (1985), Surface deformation due to shear and tensile faults in a half-space, *Bull. Seismol. Soc. Am.*, *75*, 1135–1154.

Pritchard, M. E., and M. Simons (2004), An InSAR-based survey of volcanic deformation in the central Andes, *Geochem. Geophys. Geosyst.*, *5*, Q02002, doi:10.1029/2003GC000610.

Ruiz, M. C., J. M. Lees, and J. B. Johnson (2006), Source constraints of Tungurahua volcano explosion events, *Bull. Volcanol.*, *68*, 480–490, doi:10.1007/s00445-005-0023-8.

Wicks, C. W., Jr., D. Dzurisin, S. Ingebritsen, W. Thatcher, Z. Lu, and J. Iverson (2002), Magmatic activity beneath the quiescent Three Sisters volcanic center, central Oregon Cascade Range, USA, *Geophys. Res. Lett.*, *29*(7), 1122, doi:10.1029/2001GL014205.

Williams, C. A., and G. Wadge (1998), The effects of topography on magma chamber deformation models: Application to Mt. Etna and radar interferometry, *Geophys. Res. Lett.*, *25*, 1549–1552, doi:10.1029/98GL01136.

Williams, C. A., and G. Wadge (2000), An accurate and efficient method for including the effects of topography in three-dimensional elastic models of ground deformation with applications to radar interferometry, *J. Geophys. Res.*, *105*, 8103–8120, doi:10.1029/1999JB900307.

Williams-Jones, G. (2003), Gravity changes and passive SO2 degassing at the Masaya caldera complex, Nicaragua, *J. Volcanol. Geotherm. Res.*, *123*, 137–160, doi:10.1016/S0377-0273(03)00033-7.

Zebker, H., F. Amelung, and S. Jonsson (2000), Remote sensing of volcano surface and internal processes using radar interferometry, in *Remote Sensing of Active Volcanism*, *Geophys. Monogr. Ser.*, vol. 116, edited by P. J. Mouginis-Mark, J. A. Crisp, and J. H. Fink, pp. 179–205, AGU, Washington, D. C.

F. Amelung, S. Baker, T. H. Dixon, and S-H. Hong, RSMAS, University of Miami, Coral Gables, FL 33124, USA.

J. Biggs, Department of Earth Sciences, University of Bristol, Bristol BS8 1TH, UK.

P. Mothes and M. Ruiz, Instituto Geofisico, Escuela Politenica Nacional, Ladrón de Guevara E11 - 253 Quito, Ecuador.